Rapid migration of Mongolian oak into southern Asian boreal forest

Yang Tang[1, 2], Enzai Du[1, 2*], Hongbo Guo[1, 2], Yang Wang[1, 2], Josep Peñuelas[3, 4], Peter B. Reich[5,6]

[1]State Key Laboratory of Earth Surface Processes and Resource Ecology, Faculty of Geographical Science, Beijing Normal University, Beijing 100875, China

[2]School of Natural Resources, Faculty of Geographical Science, Beijing Normal University, Beijing 100875, China

[3]CSIC, Global Ecology Unit CREAF-CSIC-UAB, 08913 Cerdanyola del Vallès, Catalonia, Spain.

[4]CREAF. 08913 Cerdanyola del Vallès, Catalonia, Spain.

[5]Institute for Global Change Biology, University of Michigan, Ann Arbor, MI, USA

[6]Department of Forest Resources, University of Minnesota, St. Paul, MN, USA

*__Corresponding author__. Enzai Du, Tel: 8610-58808085; Email: enzaidu@bnu.edu.cn

Abstract:

The migration of trees induced by climatic warming has been observed at many alpine treelines and boreal-tundra ecotones, but the migration of temperate trees into southern boreal forest remains less-well documented. We conducted a field investigation across an ecotone of temperate and boreal forests in northern Greater Khingan Mountains of northeast China. Our analysis demonstrates that Mongolian oak (*Quercus mongolica*), an important temperate tree species, has migrated rapidly into southern boreal forest in synchrony with significant climatic warming over the past century. The average rate of migration is estimated to be 12.0 ± 1.0 km decade^{-1}, which is the highest observed among migratory temperate trees (average rate 4.0 ± 1.0 km decade^{-1}) and significantly higher than the rates of tree migration at boreal-tundra ecotones (0.9 ± 0.4 km decade^{-1}) and alpine treelines (0.004 ± 0.003 km decade^{-1}). Compared with the coexisting dominant boreal tree species, Dahurian larch (*Larix gmelinii*), temperate Mongolian oak is observed to have significantly lower capacity for light acquisition, comparable water-use efficiency but stronger capacity to utilize nutrients especially the most limiting nutrient, nitrogen. In the context of climatic warming, and in addition to a high seed dispersal capacity and potential thermal niche differences, the advantage of nutrient utilization, reflected by foliar elementomes and stable nitrogen isotope ratios, is also likely a key mechanism for Mongolian oak to coexist with Dahurian larch and facilitate its migration towards boreal forest. These findings highlight a rapid deborealization of southern Asian boreal forest in response to climatic warming.

KEYWORDS

climatic warming, elemental niche, Mongolian oak, temperate-boreal forest ecotone, niche differentiation, tree migration, the Greater Khingan Mountains

1. INTRODUCTION

Climatic warming has been unprecedented at mid- to high latitudes and is projected to continue throughout the 21st century (Pörtner et al., 2022). A warmer climate affects many demographic processes of plants such as growth, mortality, reproduction, and establishment of seedlings, and therefore may result in species migration into previously colder habitats where they might out-compete previously dominant taxa (Fisichelli et al., 2012; McDowell et al., 2011; Reich et al.,

2022; Root et al., 2003; Walther et al., 2002). Field observations indicate that climatic warming has often contributed to a poleward or upward migration of many tree species (Dial et al., 2022; Du et al., 2018; Fei et al., 2017; Parmesan & Yohe, 2003; Peñuelas & Boada, 2003; Rees et al., 2020). Previous studies have mostly focused on forest vs. non-forest ecotones, such as the boreal forest-tundra ecotone and alpine treelines, where plant growth and reproduction are strongly limited by cold temperatures (Körner & Paulsen, 2004; Liang et al., 2016; Myers-Smith et al., 2015; Rees et al., 2020; Wang et al., 2016). Similarly, temperate trees are also predicted to shift their northern or upper boundaries under climatic warming and consequently alter the species composition and ecosystem function of adjacent southern boreal forest (Beckage et al., 2008; Boisvert-Marsh & de Blois, 2021; Brice et al., 2020; Kelly & Goulden, 2008; Taylor et al., 2017). The warming-induced migration of temperate trees at the temperate-boreal forest ecotone, however, remains less-well understood (Evans & Brown, 2017; Goldblum & Rigg, 2010) and different studies have had conflicting views of whether and how fast it is occurring (Ni & Vellend, 2021).

Unlike the migration of trees into the treeless arctic or alpine tundra, the northward migration of temperate trees occurs in a different context of a milder climate and better soil conditions in the southern boreal forest (Boisvert-Marsh & de Blois, 2021). These more favorable conditions (for growth and thus reproduction and dispersal) imply a potentially higher maximum rate of migration of temperate trees into southern boreal forest under climatic warming. However, the establishment of migratory temperate trees also depends on successful colonization and coexistence with and/or outcompeting the resident boreal trees (Collin et al., 2017; Delory et al., 2021; Godsoe et al., 2017; Solarik et al., 2020). The migration of northern temperate trees under climatic warming can therefore be constrained by a biological barrier of southern boreal trees, i.e., a negative biotic interaction (e.g., competition for resources) between the migrators and residents occurring at their common range boundary (Godsoe et al., 2017; Solarik et al., 2020). Although thermal and/or plant-herbivore niche differences can contribute to and/or regulate competitive rankings (Fisichelli et al., 2012; Reich et al., 2022), resource niche differentiation, i.e., different strategies for the use of light, water and nutrients, are additional key mechanisms for overcoming such biological barriers (Kraft et al., 2008; Silvertown, 2004; Tedersoo et al., 2020), but these hypothesized mechanisms have not been well elucidated for coexisting temperate and boreal trees.

Resource niche differentiation is conventionally quantified by comparing the species-specific capacity to acquire and/or use various resources (e.g., light, water, and nutrients) (Silvertown, 2004). For example, taller trees can acquire more light than shorter ones, and thus perform better under interspecific than intraspecific competition (Williams et al., 2021), so relative growth rate is a useful indicator for the differential capacity to acquire light among tree species (Falster & Westoby, 2003; King, 1981; Reich et al., 1998). Coexisting species may have different strategies for the use of water and have variable water-use efficiencies, especially in regions subject to water stress (Kulmatiski et al., 2019; Silvertown et al., 2015). Moreover, differentiation in nitrogen-use strategies in nitrogen-limited boreal forest likely facilitates species coexistence and/or determines success in interspecific competition (Du et al., 2020; McKane et al., 2002). Based on, but expanding upon, these approaches, the concept of elemental niche has been proposed to define the species-specific niche in a multidimensional space on the basis of foliar elementomes (i.e., the composition of essential elements, such as macronutrients and micronutrients) which reflect different species-specific needs and use of bioelements in amounts and proportions to adapt to different abiotic and biotic environments (Peñuelas et al., 2019; Sardans et al., 2021). Considering that the newly arrived young temperate trees under the canopy of southern boreal forest are less competitive in terms of acquiring light (Fukami, 2015), the key mechanisms for their survival likely include stronger capacities to utilize nutrients, especially nitrogen that widely limits growth of boreal trees (Högberg et al., 2017; Lambers et al., 2013; Xing et al., 2022). This hypothesis is consistent with experimental work showing that intrinsically slower growing less light competitive but more shade-tolerant species could maintain relative canopy position or even reverse height growth rankings with intrinsically faster growing *Larix* neighbors when resources were more abundant, such as in lower density neighborhoods (Boyden et al., 2009).

Boreal forest in northern Greater Khingan Mountains of northeast China, a component of the southernmost Asian Taiga (Olson et al., 2001; Su et al., 2020), has experienced significant climatic warming for decades (Pörtner et al., 2022). Field observations, manipulative experiments, and climate-vegetation models suggest better regeneration and growth in this region of Mongolian oak, a dominant tree species in adjacent northern temperate forest (Leng et al., 2006; Sun, 1998; Xu et al., 2022; Zhou et al., 2002). This evidence implies a potential migration of Mongolian oak into the southern Asian boreal forest (Leng et al., 2006; Xu et al., 2022). However, the rate of migration and possible mechanisms remain unknown. Based on a field investigation of a temperate-boreal forest ecotone in a direction approximately perpendicular to isotherms in northern Greater Khingan

Mountain, northeast China (see MATERIALS and METHODS; Figure 1a−c), we estimated the rate of migration of Mongolian oak and examined the underlying mechanisms to overcome the biological barrier of boreal Dahurian larch (*Larix gmelinii*), the dominant tree species of the regional boreal forest. Specifically, we tested two hypotheses: (*i*) Mongolian oak migrates into the boreal forest in response to climatic warming at a higher rate than do tree species at colder boreal-tundra ecotones and alpine treelines, and (*ii*) the advantage to utilize essential nutrients, especially nitrogen, facilitates Mongolian oak to coexist with and overcome the biological barrier of Duharian larch.

2. MATERIALS and METHODS

2.1 Study area and studied species

The northern Greater Khingan Mountain region (50°10′ to 53°27′ N and 119°36′ to 126°37′ E) of Northeast China is located in the southernmost edge of Eurasian boreal forest (Olson et al., 2001). This region is characterized by continental monsoon climate with long cold winter and short warm summer. About 70% of the annual precipitation occurs in summer. This region contains a large area of boreal forest with Dahurian larch (*Larix gmelinii*) as the dominant tree species (Su et al., 2020), transitioning to northern temperate forest with Mongolian oak (*Quercus mongolica*) as a dominant tree species. The soil parental material is gneiss or granite bedrock. This region is characterized by brown coniferous forest soils with an organic layer of 5−8 cm depth (Xiao & Shu, 1988). The mineral soil layer shows a depth of 20 to 40 cm with pH varying from 4.5 to 6.5 (Shi et al., 2019). Before the 20th century, the Greater Khingan Mountain region was rarely disturbed by anthropogenic activities due to the harsh climatic conditions and the rigorous ‘policy of prohibition’ (during 1650s−1900s) (Jin et al., 1991). During the past century (1920s−now), the forest ecosystems were partly disturbed due to human activities, such as hunting and logging (Jin et al., 1991). Forest fire is infrequent due to fire-prevention polices and fire-suppressing activities (Chang et al., 2007). Some grazers are found in this region, such as Siberian Roe Deer (*Capreolus pygargus*) and Red squirrel (*Sciurus Vulgaris*), mainly feeding on plant twigs, leaves and seeds.

Mongolian oak and Dahurian larch are ecologically distinct in several aspects. Mongolian oak is an initially fast but overall slowly growing tree species with intermediate shade-tolerance that generally reaches 3−9 m in height and begins sexual reproduction at 15−20 years old(Chen et al., 2017; Xu et al., 2022; Zheng et al., 1986). However, Mongolian oak trees grow slowly at their northmost distribution edge (e.g., the northern part of the Greater Khingan Mountains) due to the poor growth conditions, such as cold climate and low soil N availability (Chen et al., 2017; Wang

et al., 2005; Xu et al., 2022; Zheng et al., 1986). Dahurian larch is a fast-growing deciduous, photophilic conifer tree species that reaches 6−10 m in height at its first maturity (about 20 years old) (Jiang, 1990; Si, 1985). Both tree species are associated with ectomycorrhizal fungi (Guo et al., 2008), while Mongolian oak has a more advanced fine root system with higher specific root length, root nitrogen content and root density (Wen, 2019). Across our sampling transect (see Section 2.2 for more details), the maximum tree height (i.e., mean height of the highest 10% trees) of Mongolian oak is lower than that of Dahurian larch (6.6 ± 3.0 m vs 20.4 ± 0.8 m). Seeds of Mongolian oak and Dahurian larch are dispersed by animals (zoochory) and wind (anemochory), respectively (Ai et al., 1985; Zhang & Liu, 2014). The maximum seed dispersal distances of Mongolian oak can approach several kilometers with animals as the principal agent (Bossema, 1979; Hao & Wu, 2012; Pesendorfer et al., 2016; Zhang & Liu, 2014). Mongolian oak population can also regenerate by sprouting from rootstocks (Fan et al., 1996). In addition, Mongolian oak trees are mainly limited to the south-slope with mid- to low elevations in the southern boreal regions, due to the fact that temperature is too low for Mongolian oak trees to regenerate and reproduce on the north slope and/or at high elevations (Zhou, 1991). More detailed information for these two tree species can be found in Table S2.

2.2 Sampling transect

The rate of tree migration can be estimated by approaches such as repeated survey, repeated photography/remote sensing and dendrochronological approach (Danby, 2011; Dial et al., 2022; Peñuelas & Boada, 2003; Shiyatov, 2003). We combined field sampling and dendrochronological analysis in view of its wide application in the studies in alpine tree-line and boreal-tundra ecotones (Dial et al., 2022; Du et al., 2018; Shiyatov, 2003; Wang et al., 2016). We first conducted a field expedition in the mid-summer of 2020 to delineate the regional boundary between pure Mongolian oak forests and the advancing edge of Mongolian oak saplings within the boreal forest. Accordingly, we selected a sampling transect approximately perpendicular (i.e., with an angle of 69.5°) to the isoline of threshold warmth index (i.e., 35 °C *month*) for Mongolian oak (see Section 2.5 more detailed information on the calculation and threshold of warmth index) on the eastern slope of the Greater Khingan Mountain, covering a distance of approximately 90 kilometers (Figure 1a, b, c & S1). This transect represents the temperate-boreal forest ecotone, extending from the colder boundary of pure Mongolian oak forests to the warmer boundary of pure Dahurian larch forests (Figure 1b). Longitude of the transect ranges from 122°42′ to 123°59′ E and the latitude ranges from

50°28′ to 50°40′ N. Moreover, the altitude gradually increases from 480 m in the east to 640 m in the west (Figure 1c).

Within this transect, we selected four specific areas: Jagdaqi, Alihe, Ganhe, and Keyihe, latterly denoted as Area1, Area2, Area3, and Area4, respectively. At each area, representative forest plots (20 m × 20 m) were established at five replicated sites where the oldest Mongolian oak population occurred, with an average distance of 1.9 ± 0.6 kilometers between them. Considering that some sampling sites in Area1 were situated near the leading edge of pure Mongolian oak forests, we designated the forest site closest to the distribution edge of pure Mongolian oak forests (Area1-1; see Table S1) as the starting point of the sampling transect. Overall, a total of 20 representative forest plots across 20 sites were investigated within the four areas along the transect. According to the Seventh National Census in 2020, the average population density is about 5.6 people per square kilometer across our sampling transect with 75−94% of the population living in small towns (National Bureau of Statistics, 2021).

2.3 Field sampling

Within each sampling plot, we collected foliar samples from six healthy trees in the upper crowns of both tree species using an averruncator. Across the transect, a total of 240 foliar samples were collected, with 120 samples obtained for each tree species, respectively. For Dahurian larch, we selected the eight largest trees in each plot and sampled two ring cores from each tree using a 5.15-mm-diameter increment borer (Haglöf Sweden, Längsele, Sweden). The tree-ring cores were obtained at breast height (~1.3 m above the ground) in two perpendicular directions (east-west and north-south). In the case of Mongolian oak, three of the largest trees and three smaller trees were chosen in each forest plot. These trees were carefully felled using a hand saw at a standard height of approximately 5 cm above the ground, allowing us to sample the stem discs. Due to the relatively small diameters of many Mongolian oak trees, tree-ring core sampling was not feasible. To gather additional data, we measured the diameter at breast height (DBH, 1.3 m) of all larch and oak trees with a height greater than 1.3 m using a diameter tape. Tree height measurements were taken for the individuals selected for ring core or stem disc sampling, using an ultrasound height distance measuring instrument (Vertex IV, Haglof, Sweden). In total, we collected 320 tree-ring cores from 160 Dahurian larch trees and 120 stem discs from 120 Mongolian oak trees across the transect. To characterize the soil properties in each plot, we collected five topsoil samples (0−10 cm depth) in each forest plot and combined them into one composite sample for subsequent laboratory analyses. Furthermore, we recorded basic geographical information including latitude, longitude, elevation,

slope, and aspect for each sampling plot (Table S1) as well as any evidence of stumps or trunks of deceased oaks.

2.4 Laboratory analysis

Foliar samples were dried in an oven at 65 °C to a constant mass and further ground in a mixer mill (MM400; RETSCH, Haan, Germany) and sieved through a 100-mesh sieve. Soil samples were air dried, manually refined by removing gravel and coarse plant debris, milled and sieved through a 100-mesh sieve. Foliar nitrogen contents were measured using an elemental analyzer (Elemental Analysis system GmbH, Hanau, Germany). Additionally, we solubilized foliar samples with 6 ml HNO_3 in a microwave digestion system (Mars6 Xpress; CEM, Matthews, USA) and diluted the digested solution with ultrapure water to 25 ml. The contents of P, K, Ca, Mg, Cu, Fe, Mn and Zn were then measured using an ICP-AES (Optima 8000; PerkinElmer, Waltham, USA). Moreover, stable carbon and nitrogen isotope abundance ($\delta^{13}C$ and $\delta^{15}N$, ‰) in foliar samples were determined using a stable isotope ratio mass spectrometer (Delta V; Thermo Fisher, Massachusetts, USA). The instruments were calibrated each nine measurements using the laboratory standards. The analytical errors of the isotope measurements were below 0.05‰ and 0.25‰ for $\delta^{13}C$ and $\delta^{15}N$, respectively. The $\delta^{13}C$ and $\delta^{15}N$ were calculated according to Equation (1),

$$\delta^{13}C \text{ or } \delta^{15}N = \left(\frac{R_{sample}}{R_{standard}} - 1\right) * 1000\,‰ \quad (1)$$

where R_{sample} is the ratio of $^{13}C/^{12}C$ or $^{15}N/^{14}N$ in the sample. $R_{standard}$ is the ratio of $^{13}C/^{12}C$ in Vienna Pee Dee Belemnite standard (Coplen, 1995; McCarroll & Loader, 2004) and $^{15}N/^{14}N$ in the atmospheric N_2.

The stem discs and tree-ring cores were air dried and sanded using progressively finer grades of sandpaper until the tree-rings were clearly identified. Tree-ring widths were measured using a LINTAB 5.0 system (RINNTECH, Heidelberg, Germany) with a precision of 0.001mm. The time series of tree-ring widths were visually cross-dated and corrected using the COFECHA program (Holmes, 1983). Cambial ages of Mongolian oak and Dahurian larch were determined according to the counts of tree-rings. Mean series intercorrelation coefficient for Mongolian oak and Dahurian larch ranged 0.55−0.58 and 0.59−0.67, respectively (Table S3). All laboratory analyses were conducted in the Analysis and Test Center, State Key Laboratory of Earth Surface Processes and Resource Ecology, Beijing Normal University.

2.5 Data on climate and temporal trend of climatic variables

Monthly data on temperature and precipitation (1960–2015) for two of the four sampling areas (i.e., Area1 and Area2) were derived from two nearby meteorological stations (i.e., about 9 km to Jiagedaqi station, and 16 km to Alihe station) (China Meteorological Data Service Center, http://data.cma.cn). Climatic data (1920–2019) for all four sampling areas were also derived from CRU TS 4.05 with a resolution of 0.5 degree (http://climexp.knmi.nl/). The monthly temperature from January to December and the mean annual temperature correlated fairly well between these two datsets for Area1 and Area2 (Pearson's coefficient varied from 0.87 to 0.97, Table S4), indicating a good precision of CRU temperature data in the study area. Monthly precipitation correlated less well between these two datasets (Pearson's coefficient ranged from 0.55 to 0.89). Using the CRU dataset, we conducted linear regression analyses to evaluate the temporal trends of warmth index (cumulative monthly temperature above 5°C) during 1920–2020 (Kira, 1948). The temporal trend of annual precipitation and growing-season precipitation (May–September) (Du & Tang, 2021) were evaluated using data from meteorological stations (Figure S3). The warmth index (WI, *℃ month*) was calculated according to Equation (2),

$$WI = \sum_{i=1}^{n} (T_n - 5) \quad (2)$$

where T_n is the monthly mean temperature that exceeded a threshold temperature (i.e., 5 ℃). A threshold warmth (WI=35 ℃ *month*) is required for seed maturity of Mongolian oak (Kaplan, 2001; Xu, 1985, 1986; Yin et al., 2013). We demonstrated the isoline of the threshold for warmth index in the past century using regional monthly temperature data (1920−2020; CRU TS 4.05) (Figure 1b and S1).

2.6 Analysis of the age structure and the year of establishment

The ages of sampled trees were estimated based on the counts of tree-rings from basal discs and tree-ring cores. Given that the basal discs of Mongolian oak were sampled close to the ground (about 5 cm), the estimated age could thus indicate the actual age of the tree stem. We further explored the age-height relationship of Mongolian oak for each of the four areas using four commonly used models, i.e., linear, quadratic, exponential and power models (Table S5). The best model with the highest determinant coefficient (R^2) and the lowest Akaike Information Criterion (AIC) was established and used to predict the ages of all individuals of Mongolian oak for the sampling plots at the five replicated sites in each area. The age structure was illustrated using a frequency histogram. The year of establishment of Mongolian oak at each plot was estimated based

on three approaches, i.e., (*i*) the age of the oldest tree, (*ii*) the mean age of the oldest three trees, and (*iii*) the mean age of the oldest 10 percent of all trees, respectively.

2.7 Estimation of migration rate of Mongolian oak and movement rate of climate threshold

Raw migration rates ($Rate_{raw}$) of Mongolian oak were estimated by the inter-area distance and the difference in establishment year of Mongolian oak according to Equation (3),

$$Rate_{raw} = Dist / \Delta Year \quad (3)$$

where Dist and ΔYear indicate the geographical distance between two adjacent sampling areas and the difference in the establishment year of Mongolian oak, respectively. Specifically, for the estimation of the migration rate of Mongolian oak, the distance (i.e., Dist) between adjacent areas was calculated as the distance between each location of the five sampling sites and the location (averaged latitudes and longitudes of the five sites) of the adjacent sampling area where Mongolian oak established earlier. Estimates of migration rates for Mongolian oak were conducted separately based on three different estimates of the establishment year, i.e., the age of the oldest tree, the mean age of the oldest three trees, and the mean age of the oldest 10 percent of all trees, respectively. Because the sampling transects showed an angle of 69.5° with the isoline of the threshold warmth index (35 ℃ *month*) for Mongolian oak (Figure 1b & S1), the migration rates (i.e., $Rate_{correct}$) were further corrected according to Equation (4),

$$Rate_{correct} = Rate_{raw} * \sin 69.5° \quad (4)$$

We also estimated the spatial moving rates of threshold warmth index (i.e., 35 ℃ *month*) using a similar method. Specifically, the distance (i.e., Dist) between adjacent areas was calculated as the distance between the location (averaged latitudes and longitudes of the five sites) of the sampling areas and the location of the adjacent sampling area where the warmth index reached the threshold (35 ℃ *month*) earlier. Difference in the years (i.e., ΔYear) for warmth index reaching 35 ℃ *month* were computed accordingly. Moving rates of threshold warmth index across the transect were hence calculated and corrected according to Equation (3) and (4), respectively. We compared the migration rates of Mongolian oak and the isoline of threshold warmth index using Wilcoxon rank-sum test.

2.8 Comparison of migration rates among and within ecotones

To more broadly compare tree migration rates among temperate-boreal forest ecotones, boreal-tundra ecotones and alpine treelines, we collected data on estimated migration rates from literature.

The migration rates of trees in alpine treelines were derived from a very recent synthesis instead of a repeated review of literature (Lu et al., 2020). To collect tree migration rate data for temperate-boreal forest ecotones and boreal-tundra ecotones, we conducted a literature survey via Web of Science (https://www.webofscience.com) and Google Scholar (https://scholar.google.com) using different combinations of the following key words: "temperate/boreal/Arctic treeline/alpine treeline" and "expansion/ migration/range/distribution/boundary shift". We only recorded the data when (*i*) the migration rate was estimated based on observed migrations or range limit shifts, (*ii*) the life form of migratory species was tree, (*iii*) the observed migration occurred at temperate-boreal forest ecotones, boreal-tundra ecotones or alpine treelines, and (*iv*) the observed migration of tree species was caused by climatic warming. For temperate-boreal forest ecotones, we identified temperate tree species following previous studies (Beckage et al., 2008; Martin et al., 2021; Reich et al., 2022; Sittaro et al., 2017; Tyree et al., 1991). Only migration rates of temperate tree species were included in our analysis, while the studies on northward retreat of southern boreal trees were excluded. We further excluded the literature results either from non-ecotones or using different approaches from our study (e.g., based on the shift in geographical center rather than the leading edge of species distribution). In addition to the migration rates originally reported in the literature, we also calculated the migration rate of temperate trees based on available information, e.g., shifts in distribution edge and the corresponding time of migration. For the same species analyzed in different studies in a same region, we calculated the mean migration rate for further analysis. Based on the newly compiled database (Table S6), we compared the migration rate of trees among temperate-boreal forest ecotones, boreal-tundra ecotones and alpine treelines using one-way ANOVA with a Scheffe post hoc test.

2.9 Evaluating niche differentiation in light, water, and nutrient utilization

The height growth rate (HGR), an indicator of the capacity to compete for light during early stages of stand development (King, 1981; Lepš, 1999; Reich et al., 1998), was calculated as the height divided by the age of the tree. Specifically, the height growth rates of Dahurian larch were estimated based on the cambium age at breast height (1.3 m) and the height of the tree minus 1.3 m. The ratio of tree height growth rate was calculated for Mongolian oak versus Dahurian larch according to Equation (5),

$$Ratio_{HGR} = HGR_{oak} / HGR_{larch} \quad (5)$$

where HGR_{oak} and HGR_{larch} indicate the growth rate of tree height of Mongolian oak and Dahurian

larch, respectively.

To evaluate the differentiation of water use, we estimated the intrinsic water use efficiency (iWUE) based on foliar ^{13}C data and calculated their ratios ($Ratio_{iWUE}$) between Mongolian oak and Dahurian larch according to Equation (6),

$$Ratio_{iWUE} = iWUE_{oak} / iWUE_{larch} \quad (6)$$

where $iWUE_{oak}$ and $iWUE_{larch}$ indicate the intrinsic water use efficiencies of Mongolian oak and Dahurian larch, respectively. Intrinsic water use efficiency was defined as the ratio between the net assimilation speed (A) of CO_2 and the stomatal conductance to water vapor (g_s). Based on the mechanisms of $\Delta^{13}C$ and its relationship with C_i/C_a, the intrinsic water use efficiency (iWUE) was calculated according to Equation (7) (McCarroll & Loader, 2004),

$$iWUE = A / g_s = \frac{C_a * (b - \Delta^{13}C)}{1.6 * (b - a)} \quad (7)$$

where the symbol a is the fractionation against $^{13}CO_2$ during diffusion through stomata (4.4‰) (O'Leary, 1981), b is the fractionation during carboxylation (27‰) (Farquhar & Richards, 1984) and C_a is the concentration of ambient CO_2 obtained from Mauna Loa records (https://gml.noaa.gov/ccgg/trends/) (Keeling et al., 2001). The values of $\Delta^{13}C_a$ were calculated according to Equation (8),

$$\Delta^{13}C = (\delta^{13}C_a - \delta^{13}C_p) * (1 + \frac{\delta^{13}C_p}{1000}) \quad (8)$$

where $\delta^{13}C_a$ and $\delta^{13}C_p$ are the isotope ratios of carbon (i.e., $^{13}C/^{12}C$) in the atmospheric CO_2 and plant (e.g., foliar samples), respectively.

Foliar $\delta^{15}N$ are indicative for plant N utilization (Amundson et al., 2003; Craine et al., 2015). To assess the differentiation in nitrogen utilization between coexisting Mongolian oak and Dahurian larch, we evaluated the N use difference (Dif_N) based on the foliar $\delta^{15}N$ according to Equations (9),

$$Dif_N = \delta^{15}N_{oak} - \delta^{15}N_{larch} \quad (9)$$

We further compared the elementomes of coexisting Mongolian oak and Dahurian larch based on the foliar contents of nine essential nutrients (N, P, K, Ca, Mg, Cu, Fe, Mn and Zn). Nutrient content data were first normalized (mean = 0, sd = 1) and then a general principal components analysis (PCA) was conducted to test the inter-specific difference of elementomes in the PCs space

(Peñuelas et al., 2010; Urbina et al., 2017). Then a paired t-test was employed to determine how PC1 and PC2 scores of elementomes differed between Mongolian oak and Dahurian larch (Peñuelas et al., 2010; Urbina et al., 2017). The elementomic distances (Euclidean) between Mongolian oak and Dahurian larch were calculated using *vegdist* function (vegan package) in R environment (Fernandez-Martinez et al., 2021; Oksanen et al., 2013). Smaller elementomic distances indicate more similar functional strategies and stronger overlap of stoichiometric niches (Fernandez-Martinez et al., 2021).

Paired t-test or Wilcoxon rank-sum test were used to compare the indicators for light acquisition (i.e., tree height growth rate), water use (i.e., water use efficiency), nitrogen (i.e., foliar $\delta^{15}N$ and N content) and nutrient use (i.e., foliar elementome) of coexisting Mongolian oak and Dahurian larch. Linear regression analyses were conducted to explore the spatial variation of indicators for interspecific differentiation in light (the ratio of tree height growth rate), water (the ratio of water use efficiency), nitrogen (Dif_N) and nutrient use (elementomic distances) across the sampling transect, respectively. All statistical analyses were performed in R 4.2.0 software with a significance level of 0.05 (R Core Team, 2015).

3. RESULTS

3.1 Significant climatic warming across the temperate-boreal forest ecotone

The warmth index in the study region increased significantly during the last nine decades ($P < 0.001$; 0.135−0.143 *℃ month* y^{-1}), especially after 1960 (Figure 1d). The warmth index at the current border of the pure temperate Mongolian oak forest (i.e., Area1) was consistently above the threshold warmth index (35 *℃ month*) for Mongolian oak throughout the recorded period. The warmth index for Area2 and Area3 approximated the threshold around 1950 while it stayed consistently below the threshold in Area4 until 1995 (Figure 1d). In the context of climatic warming, the front border of the threshold warmth index (i.e., 35 *℃ month*) moved towards the boreal forest at an average rate of 14.7 ± 3.5 km $decade^{-1}$ across the transect (Figure S2). Both annual precipitation and growing-season precipitation (i.e., May–September) (Du & Tang, 2021) had no significant trends during the same period ($P > 0.05$; Figure S3).

3.2 Rapid migration of Mongolian oak into the southern Asian boreal forest

The age structures of Mongolian oak in the five repeated forest plots were generally more similar within each area than among them (Figure 2) and the maximum ages of the oak trees decreased

significantly towards the boreal forest ($p<0.001$; Figures 3a). Mongolian oak was estimated to establish in Area1 around 1924, arrive at Area2 and Area3 in 1955 and 1975, respectively, and reach the current leading edge, i.e., Area4, around 2000 (Figure 2a). Based on the three oldest trees in each plot, we estimated that Mongolian oak migrated into the southern boreal forest at an average rate of 12.0 ± 1.0 km decade^{-1} (Figure 3c). The migration rates estimated using the ages of the oldest tree and the oldest 10% of all oak trees were similar (Figure 3b & 3d). This migration rate is rapid compared to those recorded elsewhere in similar contexts; in fact, it is the highest rate of migration for a temperate tree species among all reported expansions of temperate conifer (e.g., white pine) and broadleaf trees (e.g., gray birch, red oak and sugar maple) into the southern boreal forest (Figure 4a; Table S6). Our further analysis shows that the rate of migration associated with climatic warming decreased significantly in the order of the ecotone of temperate-boreal forest (4.0 ± 1.0 km decade^{-1}) > boreal-tundra ecotones (0.9 ± 0.4 km decade^{-1}) > alpine treelines (0.004 ± 0.003 km decade^{-1}) ($P < 0.05$; Figure 4b and Table S6). Thus, the migration of Mongolian oak is extremely rapid among multiple high latitude biomes and contexts (the highest for the fastest migrating group).

3.3 Performance and niche differentiation between Mongolian oak and Dahurian larch

The height growth rate of Mongolian oak was significantly lower than that of Dahurian larch, implying a lower light acquisition capacity of Mongolian oak ($t_{19} = 56.27$, $P < 0.01$; Figure 5a). The ratio of the height growth rate of Mongolian oak versus Dahurian larch decreased significantly toward the southern boreal forest ($P < 0.05$; Figure 5b). Intrinsic water-use efficiency did not differ significantly between these two species ($t_{19} = -1.64$, $P = 0.12$; Figure 5c), and the ratio of the water-use efficiencies showed no significant trend across the transect ($P = 0.46$; Figure 5d). The foliar $\delta^{15}N$ was significantly lower for Mongolian oak than Dahurian larch ($t_{19} = 2.13$, $P < 0.05$; Figure 5e). The difference in foliar $\delta^{15}N$ (Nif_N) between these two species increased significantly toward the southern boreal forest ($P < 0.05$; Figure 5f), suggesting consistently higher capacity of Mongolian oak to utilize nitrogen that significantly limits the growth of Dahurian larch (Xing et al., 2022).

Principal component analysis (PCA) of leaf elements suggests significant differentiation between Mongolian oak and Dahurian larch on the PC1 axis ($W = 0$, $P < 0.01$; Figures 5g & S4 and Table S7). The PC1 axis was closely associated with the variation of the foliar contents of N, P, Ca, Mg and Cu and explained 43.1% of the total variance of the elemental contents (Figures 5g

412 & S4, Table S7). The variations of the foliar contents of K, Fe and Mn along the PC2 axis also
413 differed significantly between the two species ($t_{19} = -2.97$, $P < 0.01$; Figures 5g & S4 and Table
414 S7) and explained 18.% of the total variance of the elemental contents (Figures 5g & S4).
415 Specifically, the foliar contents of N, P, Ca, Mg, and Mn were significantly higher for Mongolian
416 oak than Dahurian larch ($P < 0.05$; Figures 5g & S5). The elementomic distances between
417 coexisting Mongolian oak and Dahurian larch increased significantly towards the southern boreal
418 forest ($P < 0.01$; Figure 5h).

419 **4. DISCUSSION**

420 **4.1 Rapid migration of Mongolian oak**

421 Our results indicate that Mongolian oak has migrated rapidly into the southern Asian boreal forest
422 during the last century, likely at least in part in response to the significant climatic warming. The
423 migration rate of Mongolian oak (i.e., 12.0 ± 1.0 km decade^{-1}) estimated in our study is comparable
424 to that of the oak trees (i.e., ~10 km decade^{-1}) migrating into Great Britain after the last glacial
425 period documented in Reid's paradox (Clark, 1998). The migration of Mongolian oak nearly kept
426 pace with the movement of threshold warmth index (35 °*C month*) across the transect (12.0 ± 1.0
427 vs 14.7 ± 3.5 km decade^{-1}; Figure S2).

428 Consistent with our first hypothesis, the migration of Mongolian oak into the boreal forest
429 was significantly faster than the migration of trees at boreal-tundra ecotones and alpine treelines,
430 where migration lags far behind the rapid climatic warming (Figure 4 and Table S7) (Lu et al.,
431 2020; McLaren et al., 2017; Payette, 2007; Rees et al., 2020). The slower migration of tree species
432 at boreal-tundra ecotones and alpine treelines may be limited by lower seed germination and
433 seedling recruitment due to the harsh climates (e.g., low temperatures, frequent frost and/or intense
434 ultraviolet radiation) and poor soil conditions (e.g., low contents of nutrients and/or availability of
435 water) (Harsch & Bader, 2011; Lenoir et al., 2008; Macias-Fauria & Johnson, 2013; Rees et al.,
436 2020). In contrast, better climatic and edaphic conditions in the southern boreal forest may partially
437 facilitate the migration of temperate trees at the temperate-boreal forest ecotone (Boisvert-Marsh
438 et al., 2019; Sittaro et al., 2017).

439 Previous studies conducted in the northern Greater Khingan Mountain region have also provided
440 evidence for the expansion of Mongolian oak into the boreal forest. Sun (1998) and Zhou et al.
441 (2002) conducted field investigations along an ecological transect at the northern distribution edge

of Mongolian oak in the northern Great Khingan mountains. Their findings revealed successful regeneration and establishment of Mongolian oak within boreal larch forest stands over the past few decades. These studies contribute further support to the understanding of Mongolian oak's migration into the boreal forest in the studied region. However, neither the migration rate of Mongolian oak nor the potential mechanisms driving its expansion, aside from the assumed role of climatic warming, were estimated or systematically explored in these studies.

4.2 Mechanisms of the migration of Mongolian oak

The migration of tree species is jointly controlled by climatic barriers (e.g., cold limitation), dispersal barriers (e.g., seed dispersal limitation, seedbed suitability and seed predation), biological barriers (e.g., competition with resident species), and their interaction (e.g., shifting competitive rankings across thermal gradients (Figure 6) (Fisichelli et al., 2012; Lambers et al., 2013; Reich et al., 2022; Reich et al., 2015). In our study region, rapid climatic warming in recent decades has resulted in a significant increase of warmth index (Figure 1d & 6a) that continuingly exceeded the assumed thermal threshold of regeneration and reproduction of oak trees beyond the previous leading edge. In view of the alleviated climatic barrier, limits to the dispersal of propagules (e.g., seeds) by animals (i.e., dispersal barrier) (Johnson & Webb III, 1989; Wall, 2001) and the biological barrier of coexisting boreal trees can control the migration success and rate of temperate trees under climatic warming (Fukami, 2015; Lambers et al., 2013; Solarik et al., 2020) (Figure 6a). Specifically, the known dispersal agents of oak acorns include sciurid and other large rodents (e.g., Red squirrels and Siberian chipmunk) and corvid birds (e.g., Eurasian jays and Eurasian nutcracker) in this region (Hao & Wu, 2012; Pesendorfer et al., 2016; Zhang & Liu, 2014), and acorns of oaks can be dispersed by these animals up to a maximum of several kilometers (Bossema, 1979; Higgins et al., 2003; Purves et al., 2007). The estimated rate of migration of Mongolian oak (12.0 ± 1.0 km decade^{-1}) falls in the range of the maximum seed dispersal rate (Figure 6b), implying that seed dispersal is not likely a strongly limiting factor for the migration of Mongolian oak; i.e., high seed dispersal capacity is likely a key mechanisms contributing to the rapid migration of Mongolian oak.

Another key mechanism for the rapid migration of Mongolian oak involves how it overcomes the biological barrier of residential boreal larch trees (Solarik et al., 2020) (Figure 6a). Our analyses revealed that Mongolian oak exhibited lower capacity for light acquisition and did not demonstrate a significant advantage in water use efficiency when compared to the coexisting Dahurian larch

(Figure 5g, S5, S7 & S8). However, Mongolian oak was shown to possess intermediate shade tolerance (Beon & Bartsch, 2003; Kweon & Comeau, 2021), allowing it to adapt to the light conditions beneath the canopy of the larch forest. In addition, the canopy of boreal larch forest allows considerable sunlight transmittance to the forest floor (Zheng et al., 1986) and this may potentially both alleviate the light limitation of young Mongolian oaks and protect them from potential photo damage of unshaded sunlight. Moreover, Mongolian oaks had stronger capacities to utilize essential nutrients, especially nitrogen, that widely limits the growth of Dahurian larch in the studied region (Xing et al., 2022). As reflected by the elementomes, higher contents of the macronutrients could favor photosynthesis and growth of Mongolian oak in competition with regenerating larch and/or native shrubs in the partially shaded understories. The advantage in utilization of limiting nutrients is likely a key mechanism for Mongolian oak to overcome the biological barrier and coexist with existing older and taller larch trees under continuing climatic warming (Figure 6), in line with our second hypothesis.

Other factors, such as disturbance, could also affect shifts in species distributions (Boisvert-Marsh & de Blois, 2021; Brice et al., 2020; Hill & Field, 2021). For instance, disturbances could directly influence the demographic processes (e.g., growth and mortality) and species turnover or indirectly provide establishment opportunities for migratory trees by creating canopy gaps (Brice et al., 2020). As one of the most important disturbances in boreal region, fire events, have neither been evidenced by the sampled tree-ring cores nor been reported previously across the studied transect (Jin et al., 1991). Furthermore, we found only few dead trees (e.g., N = 17 and mean DBH= 4.6 ± 2.2 cm) and stumps of Mongolian oak across the transect during the field expedition and investigation. This refutes the idea of a dominant role of species infilling or turnover induced by disturbances in shaping the significant age trends of Mongolian oak relative dominance to migrating into the boreal forest. Overall, the spatial trends of tree age and relative basal area of Mongolian oak (Figures 3a & S6) across the temperate-boreal forest ecotone most likely result from the species migration under climatic warming.

4.3 Implications and future research needs

Tree-ring studies in the southern Asian boreal forest have suggested a growth decline of Dahurian larch in response to recent climatic warming (Bai et al., 2019; Li et al., 2020; Li et al., 2023). For instance, a recent analysis of large-scale networks of tree ring data (i.e., the International Tree-Ring Data Bank, ITRDB) suggests that rapid climatic warming has induced widespread growth

decline of Dahurian larch in the southern Asian boreal forest mainly as a result of the warming-induced drought stress (Li et al., 2023). Specifically, the maximum temperature during the growing season (generally > 20℃) has exceeded the physiological optimum temperature for Dahurian larch (15−20 ℃) in the southern boreal regions (Huang et al., 2019), which would likely result in a decline in foliar photosynthetic productivity (Medlyn et al., 2002). On the contrary, climatic warming has been found to significantly enhance the growth of temperate oak trees and several other temperate trees in temperate-boreal ecotones (Fisichelli et al., 2012; Goldblum & Rigg, 2005; Reich et al., 2022; Reich et al., 2015; Zhou et al., 2002). The potentially distinct growth responses of larch and oak trees to climatic warming imply that warmer temperatures in the future may further weaken the biological barrier for the migration of Mongolian oak. In this context, the migration of Mongolian oak will likely continue, which may consequently trigger a major change in the ecosystem structure and functioning of the southern Asian boreal forest. Therefore, further research efforts are needed to reveal the ecological and biogeochemical impacts of temperate tree migration on the southern Asian boreal forest.

Additionally, the analysis of the elemental niche indicates a greater capacity for nutrient utilization by Mongolian oak compared to boreal Dahurian larch (Figure 5 & S7 & S8). This could potentially promote the establishment of Mongolian oak and its coexistence with Dahurian larch in the southern boreal forest, characterized by low soil nutrient availability. To further validate this mechanism, experimental nutrient manipulations, such as varying levels of nitrogen addition, are required to assess how nutrient availability affects the colonization and growth of Mongolian oak in boreal forest stands. Furthermore, with future climate warming expected to accelerate nutrient cycling and enhance nitrogen availability in the southern boreal forest, these experimental efforts are likely to provide insights into the future migration of Mongolian oak and its interaction with boreal trees in the context of climate change.

5. Conclusions

Based on a systematic field investigation across a temperate-boreal forest ecotone in the northern Great Khingan mountains in Northeast China, we estimated the rate of migration of Mongolian oak and evaluated potential mechanisms. Our findings suggested that temperate Mongolian oak has migrated rapidly toward the southern Asian boreal forest and kept pace with significant climatic warming during the past century. Key mechanisms underlying the rapid migration of Mongolian oak include relatively long distance seed dispersal capacity, potential thermal niche

differences and the ability of migratory Mongolian oak to co-exist with Dahurian larch, and thus overcome a biological barrier to migration. This latter ability likely involves its advantage to nutrient utilization, especially for the limiting nitrogen, reflected by foliar elementomes and stable nitrogen isotope ratio. Overall, these findings highlight a rapid deborealization of southern Asian boreal forest in this region in response to climatic warming.

ACKNOWLEDGMENTS

We are grateful for the financial support from the Science and Technology Key Project of Inner Mongolia Autonomous Region, China (2021ZD0011), National Natural Science Foundation of China (41877328&41630750), and the State Key Laboratory of Earth Surface Processes and Resource Ecology (2021-TS-02). JP research was supported by the Spanish Government grant TED2021-132627B-I00 funded by MCIN, AEI/10.13039/501100011033 and the European Union NextGenerationEU/PRTR, the Fundación Ramón Areces grant CIVP20A6621, and the Catalan Government grant SGR2021-1333. PR research was supported by Biological Integration Institutes award NSF-DBI-2021898. We thank Dr. Yingna Liu, Dr. Xiaofei Gao, Dr. Xin Wei, Dr. Yingying Liu, Yuying Guo, Yuehan Tian, Xinlian Zhang, Yaqi Li, Shi Li, Yue Song, Haixing Wang, Zhu Zhu and Zixuan Zheng for their assistance of the laboratory analysis. We also acknowledge the authors whose research was included in the literature-reviewed dataset in this manuscript.

AUTHOR CONTRIBUTIONS

E.D. conceived the project. Y.T., E.D., H.G. and Y.W. performed the field sampling, laboratory measurements and statistical analyses. E.D., Y.T., J.P. and P.R. interpreted the data patterns, evaluated competing hypotheses, and wrote and revised the manuscript.

COMPETING INTERESTS

The authors declare no competing interests.

DATA AND MATERIALS AVALABILITY

All data used for this study are available in Figshare (https://doi.org/10.6084/m9.figshare.22650253.v2).

REFFERENCES

Ai, C., Wang, S., & Ai, S. (1985). Study on the seed dispersal of Larix gmelini. *Forestry Science Technology, 4*, 2-5 (in Chinese).

Amundson, R., Austin, A. T., Schuur, E. A. G., Yoo, K., Matzek, V., Kendall, C., Uebersax, A., Brenner, D., & Baisden, W. T. (2003). Global patterns of the isotopic composition of soil and plant nitrogen. *Global Biogeochemical Cycles, 17*(1), 1031.

Bai, X., Zhang, X., Li, J., Duan, X., Jin, Y., & Chen, Z. (2019). Altitudinal disparity in growth of Dahurian larch (Larix gmelinii Rupr.) in response to recent climate change in northeast China. *Science of The Total Environment, 670*, 466-477.

Beckage, B., Osborne, B., Gavin, D. G., Pucko, C., Siccama, T., & Perkins, T. (2008). A rapid upward shift of a forest ecotone during 40 years of warming in the Green Mountains of Vermont. *Proceedings of the National Academy of Sciences, 105*(11), 4197-4202.

Beon, M.-S., & Bartsch, N. (2003). Early seedling growth of pine (Pinus densiflora) and oaks (Quercus serrata, Q. mongolica, Q. variabilis) in response to light intensity and soil moisture. *Plant Ecology, 167*, 97-105.

Boisvert-Marsh, L., & de Blois, S. (2021). Unravelling potential northward migration pathways for tree species under climate change. *Journal of Biogeography, 48*(5), 1088-1100.

Boisvert-Marsh, L., Périé, C., & de Blois, S. (2019). Divergent responses to climate change and disturbance drive recruitment patterns underlying latitudinal shifts of tree species. *Journal of Ecology, 107*(4), 1956-1969.

Bossema, I. (1979). Jays and oaks: an eco-ethological study of a symbiosis. *Behaviour, 70*(1-2), 1-116.

Boyden, S. B., Reich, P. B., Puettmann, K. J., & Baker, T. R. (2009). Effects of density and ontogeny on size and growth ranks of three competing tree species. *Journal of Ecology, 97*(2), 277-288.

Brice, M. H., Vissault, S., Vieira, W., Gravel, D., Legendre, P., & Fortin, M. J. (2020). Moderate disturbances accelerate forest transition dynamics under climate change in the temperate–boreal ecotone of eastern North America. *Global Change Biology, 26*(8), 4418-4435.

Chang, Y., He, H., Bishop, I., Hu, Y., Bu, R., Xu, C., & Li, X. (2007). Long-term forest landscape responses to fire exclusion in the Great Xing'an Mountains, China. *International Journal of Wildland Fire, 16*(1), 34-44.

Chen, L., Chen, J., Zhang, Q., Wang, J., & Zhang, W. (2017). The Quercus mongolica growth process research of different community in forest district of Jiaohe. *Journal of Jilin Forestry Science and Technology, 46*(6), 9-14 (in Chinese).

Clark, J. S. (1998). Why trees migrate so fast: confronting theory with dispersal biology and the paleorecord. *The American Naturalist, 152*(2), 204-224.

Collin, A., Messier, C., & Belanger, N. (2017). Conifer presence may negatively affect sugar maple's ability to migrate into the boreal forest through reduced foliar nutritional status. *Ecosystems, 20*(4), 701-716.

Coplen, T. B. (1995). Discontinuance of SMOW and PDB. *Nature, 375*(6529), 285-285.

Craine, J. M., Brookshire, E. N. J., Cramer, M. D., Hasselquist, N. J., Koba, K., Marin-Spiotta, E., & Wang, L. (2015). Ecological interpretations of nitrogen isotope ratios of terrestrial plants and soils. *Plant and Soil, 396*(1), 1-26.

Danby, R. K. (2011). Monitoring forest–tundra ecotones at multiple scales. *Geography Compass, 5*(9), 623-640.

Delory, B. M., Schempp, H., Spachmann, S. M., Störzer, L., van Dam, N. M., Temperton, V. M., & Weinhold, A. (2021). Soil chemical legacies trigger species-specific and context-dependent root responses in later arriving plants. *Plant, Cell & Environment, 44*(4), 1215-1230.

Dial, R. J., Maher, C. T., Hewitt, R. E., & Sullivan, P. F. (2022). Sufficient conditions for rapid range expansion of a boreal conifer. *Nature, 608*(7923), 546-551.

Du, E., & Tang, Y. (2021). Distinct climate effects on Dahurian Larch growth at an Asian temperate-boreal forest ecotone and nearby boreal sites. *Forests, 13*(1), 27.

Du, E., Terrer, C., Pellegrini, A. F. A., Ahlström, A., van Lissa, C. J., Zhao, X., Xia, N., Wu, X., & Jackson, R. B. (2020). Global patterns of terrestrial nitrogen and phosphorus limitation. *Nature Geoscience, 13*(3), 221-226.

Du , H., Liu, J., Li, M. H., Büntgen, U., Yang, Y., Wang, L., Wu, Z., & He, H. S. (2018). Warming‐induced upward migration of the alpine treeline in the Changbai Mountains, northeast China. *Global Change Biology, 24*(3), 1256-1266.

Evans, P., & Brown, C. D. (2017). The boreal–temperate forest ecotone response to climate change. *Environmental Reviews, 25*(4), 423-431.

Falster, D. S., & Westoby, M. (2003). Plant height and evolutionary games. *Trends in Ecology & Evolution*, *18*(7), 337-343.
Fan, H., Li, D., & Zang, R. (1996). Natural regeneration of Mongolian Oak population. *Chinese Journal of Ecology*, *3*, 15-20 (in Chinese).
Farquhar, G. D., & Richards, R. A. (1984). Isotopic composition of plant carbon correlates with water-use efficiency of wheat genotypes. *Functional Plant Biology*, *11*(6), 539-552.
Fei, S., Desprez, J. M., Potter, K. M., Jo, I., Knott, J. A., & Oswalt, C. M. (2017). Divergence of species responses to climate change. *Science Advances*, *3*(5), e1603055.
Fernandez-Martinez, M., Preece, C., Corbera, J., Cano, O., Garcia-Porta, J., Sardans, J., Janssens, I. A., Sabater, F., & Peñuelas, J. (2021). Bryophyte C:N:P stoichiometry, biogeochemical niches and elementome plasticity driven by environment and coexistence. *Ecology Letters*, *24*(7), 1375-1386.
Fisichelli, N., Frelich, L. E., & Reich, P. B. (2012). Sapling growth responses to warmer temperatures 'cooled'by browse pressure. *Global Change Biology*, *18*(11), 3455-3463.
Fukami, T. (2015). Historical contingency in community assembly: integrating niches, species pools, and priority effects. *Annual Review of Ecology, Evolution, and Systematics*, *46*, 1-23.
Godsoe, W., Jankowski, J., Holt, R. D., & Gravel, D. (2017). Integrating biogeography with contemporary niche theory. *Trends in Ecology & Evolution*, *32*(7), 488-499.
Goldblum, D., & Rigg, L. S. (2005). Tree growth response to climate change at the deciduous boreal forest ecotone, Ontario, Canada. *Canadian Journal of Forest Research*, *35*(11), 2709-2718.
Goldblum, D., & Rigg, L. S. (2010). The deciduous forest–boreal forest ecotone. *Geography Compass*, *4*(7), 701-717.
Guo, D., Xia, M., Wei, X., Chang, W., Liu, Y., & Wang, Z. (2008). Anatomical traits associated with absorption and mycorrhizal colonization are linked to root branch order in twenty‐three Chinese temperate tree species. *New Phytologist*, *180*(3), 673-683.
Hao, H., & Wu, J. (2012). The role of Squirrel in the dispersal of Mongolian Oak in the Northeast Forestry University Forestry farm in Harbin. *Territory & Natural Resources Study*, *4*, 84-85 (in Chinese).
Harsch, M. A., & Bader, M. Y. (2011). Treeline form–a potential key to understanding treeline dynamics. *Global Ecology and Biogeography*, *20*(4), 582-596.
Higgins, S. I., Nathan, R., & Cain, M. L. (2003). Are long-distance dispersal events in plants usually caused by nonstandard means of dispersal? *Ecology*, *84*(8), 1945-1956.
Hill, A. P., & Field, C. B. (2021). Forest fires and climate-induced tree range shifts in the western US. *Nature Communications*, *12*(1), 6583.
Högberg, P., Näsholm, T., Franklin, O., & Högberg, M. N. (2017). Tamm Review: On the nature of the nitrogen limitation to plant growth in Fennoscandian boreal forests. *Forest Ecology and Management*, *403*, 161-185.
Holmes, R. L. (1983). Computer assisted quality control in tree-ring dating and measurement. *Tree-Ring Bulletin*, *43*, 69-78.
Huang, M., Piao, S., Ciais, P., Peñuelas, J., Wang, X., Keenan, T. F., Peng, S., Berry, J. A., Wang, K., & Mao, J. (2019). Air temperature optima of vegetation productivity across global biomes. *Nature Ecology & Evolution*, *3*(5), 772-779.
Jiang, Y. L., Fengri; Li, Changsheng. (1990). Growth and yield of young and middle age stands of Darhuian larch. *Journal of North-East Forestry University*, *18*(1), 1-7.
Jin, X., Zhang, R., & Feng, G. (1991). *Chorography of Oroqen Autonomous Banner*. Inner Mongolia People's Publishing House, Hohhot.
Johnson, W. C., & Webb III, T. (1989). The role of blue jays (Cyanocitta cristata L.) in the postglacial dispersal of fagaceous trees in eastern North America. *Journal of Biogeography*, 561-571.
Kaplan, J. O. (2001). *Geophysical applications of vegetation modeling* [Doctoral dissertation]. Lund University.
Keeling, C. D., Piper, S. C., Bacastow, R. B., Wahlen, M., Whorf, T. P., Heimann, M., & Meijer, H. A. (2001). Exchanges of atmospheric CO2 and 13CO2 with the terrestrial biosphere and oceans from 1978 to 2000. I. Global Aspects. SIO Reference Series, No. 01–06. San Diego: Scripps Institution of Oceanography.
Kelly, A. E., & Goulden, M. L. (2008). Rapid shifts in plant distribution with recent climate change. *Proceedings of the National Academy of Sciences*, *105*(33), 11823-11826.
King, D. (1981). Tree dimensions: maximizing the rate of height growth in dense stands. *Oecologia*, *51*(3), 351-356.
Kira, T. (1948). On the altitudinal arrangement of climatic zones in Japan. *Kanti-Nougaku*, *2*, 143-173.
Körner, C., & Paulsen, J. (2004). A world-wide study of high altitude treeline temperatures. *Journal of Biogeography*, *31*(5), 713-732.
Kraft, N. J., Valencia, R., & Ackerly, D. D. (2008). Functional traits and niche-based tree community assembly in an Amazonian forest. *Science*, *322*(5901), 580-582.

673 Kulmatiski, A., Adler, P. B., Foley, K. M., & Schwinning, S. (2019). Hydrologic niches explain species coexistence
674 and abundance in a shrub–steppe system. *Journal of Ecology, 108*(3), 998-1008.
675 Kweon, D., & Comeau, P. G. (2021). Climate, site conditions, and stand characteristics influence maximum size-
676 density relationships in Korean red pine (Pinus densiflora) and Mongolian oak (Quercus mongolica) stands,
677 South Korea. *Forest Ecology and Management, 502*, 119727.
678 Lambers, J. H. R., Harsch, M. A., Ettinger, A. K., Ford, K. R., & Theobald, E. J. (2013). How will biotic interactions
679 influence climate change–induced range shifts? *Annals of the New York Academy of Sciences, 1297*(1), 112-
680 125.
681 Leng, W., He, H., Bu, R., & Hu, Y. (2006). The spatial distribution of constructive species of Northeast forest under
682 the climate changing. *Acta Ecologica Sinica, 26*(12), 4257-4266 (in Chinese).
683 Lenoir, J., Gégout, J. C., Marquet, P. A., de Ruffray, P., & Brisse, H. (2008). A significant upward shift in plant
684 species optimum elevation during the 20th century. *Science, 320*(5884), 1768-1771.
685 Lepš, J. (1999). Nutrient status, disturbance and competition: an experimental test of relationships in a wet meadow.
686 *Journal of Vegetation Science, 10*(2), 219-230.
687 Li, W., Jiang, Y., Dong, M., Du, E., Zhou, Z., Zhao, S., & Xu, H. (2020). Diverse responses of radial growth to climate
688 across the southern part of the Asian boreal forests in northeast China. *Forest Ecology and Management,*
689 *458*, 117759.
690 Li, W., Manzanedo, R. D., Jiang, Y., Ma, W., Du, E., Zhao, S., Rademacher, T., Dong, M., Xu, H., & Kang, X. (2023).
691 Reassessment of growth-climate relations indicates the potential for decline across Eurasian boreal larch
692 forests. *Nature Communications, 14*(1), 3358.
693 Liang, E., Wang, Y., Piao, S., Lu, X., Camarero, J. J., Zhu, H., Zhu, L., Ellison, A. M., Ciais, P., & Penuelas, J. (2016).
694 Species interactions slow warming-induced upward shifts of treelines on the Tibetan Plateau. *Proceedings of*
695 *the National Academy of Sciences, 113*(16), 4380-4385. doi:10.1073/pnas.1520582113
696 Lu, X., Liang, E., Wang, Y., Babst, F., Camarero, J. J., & Grytnes, J. A. (2020). Mountain treelines climb slowly
697 despite rapid climate warming. *Global Ecology and Biogeography, 30*(1), 305-315.
698 Macias-Fauria, M., & Johnson, E. A. (2013). Warming-induced upslope advance of subalpine forest is severely limited
699 by geomorphic processes. *Proceedings of the National Academy of Sciences of the United States of America,*
700 *110*(20), 8117-8122.
701 Martin, M., Woodbury, D., Glogower, Y., Duguid, M., Frey, B., & Ashton, M. (2021). Within-gap position shapes
702 fifty years of forest dynamics in a temperate hardwood forest in Connecticut, USA. *Forest Ecology and*
703 *Management, 494*, 119311.
704 McCarroll, D., & Loader, N. J. (2004). Stable isotopes in tree rings. *Quaternary Science Reviews, 23*(7-8), 771-801.
705 McDowell, N. G., Beerling, D. J., Breshears, D. D., Fisher, R. A., Raffa, K. F., & Stitt, M. (2011). The interdependence
706 of mechanisms underlying climate-driven vegetation mortality. *Trends in Ecology & Evolution, 26*(10), 523-
707 532.
708 McKane, R. B., Johnson, L. C., Shaver, G. R., Nadelhoffer, K. J., Rastetter, E. B., Fry, B., Giblin, A. E., Kielland, K.,
709 Kwiatkowski, B. L., & Laundre, J. A. (2002). Resource-based niches provide a basis for plant species
710 diversity and dominance in arctic tundra. *Nature, 415*(6867), 68-71.
711 McLaren, J. R., Buckeridge, K. M., van de Weg, M. J., Shaver, G. R., Schimel, J. P., & Gough, L. (2017). Shrub
712 encroachment in Arctic tundra: Betula nana effects on above-and belowground litter decomposition. *Ecology*,
713 *98*(5), 1361-1376.
714 Medlyn, B. E., Dreyer, E., Ellsworth, D., Forstreuter, M., Harley, P. C., Kirschbaum, M. U. F., Le Roux, X., Montpied,
715 P., Strassemeyer, J., & Walcroft, A. (2002). Temperature response of parameters of a biochemically based
716 model of photosynthesis. II. A review of experimental data. *Plant, Cell & Environment, 25*(9), 1167-1179.
717 Myers-Smith, I. H., Elmendorf, S. C., Beck, P. S., Wilmking, M., Hallinger, M., Blok, D., Tape, K. D., Rayback, S.
718 A., Macias-Fauria, M., & Forbes, B. C. (2015). Climate sensitivity of shrub growth across the tundra biome.
719 *Nature Climate Change, 5*(9), 887-891.
720 National Bureau of Statistics. (2021). Communique of the Seventh National Population Census.
721 http://www.stats.gov.cn/tjsj/.
722 Ni, M., & Vellend, M. (2021). Space-for-time inferences about range-edge dynamics of tree species can be influenced
723 by sampling biases. *Global Change Biology, 27*(10), 2102-2112.
724 O'Leary, M. H. (1981). Carbon isotope fractionation in plants. *Phytochemistry, 20*(4), 553-567.
725 Oksanen, J., Blanchet, F. G., Kindt, R., Legendre, P., Minchin, P. R., O'hara, R. B., Simpson, G. L., Solymos, P.,
726 Stevens, M. H. H., & Wagner, H. (2013). Package 'vegan'. *Community ecology package, version, 2*(9), 1-
727 295.
728 Olson, D. M., Dinerstein, E., Wikramanayake, E. D., Burgess, N. D., Powell, G. V., Underwood, E. C., D'amico, J.
729 A., Itoua, I., Strand, H. E., & Morrison, J. C. (2001). Terrestrial ecoregions of the world: a new map of life

on Earth: a new global map of terrestrial ecoregions provides an innovative tool for conserving biodiversity. *BioScience, 51*(11), 933-938.
Parmesan, C., & Yohe, G. (2003). A globally coherent fingerprint of climate change impacts across natural systems. *Nature, 421*(6918), 37-42.
Payette, S. (2007). Contrasted dynamics of northern Labrador tree lines caused by climate change and migrational lag. *Ecology, 88*(3), 770-780.
Peñuelas, J., & Boada, M. (2003). A global change-induced biome shift in the Montseny mountains (NE Spain). *Global Change Biology, 9*(2), 131-140.
Peñuelas, J., Fernández-Martínez, M., Ciais, P., Jou, D., Piao, S., Obersteiner, M., Vicca, S., Janssens, I. A., & Sardans, J. (2019). The bioelements, the elementome, and the biogeochemical niche. *Ecology, 100*(5), e02652.
Peñuelas, J., Sardans, J., Llusià, J., Owen, S. M., Carnicer, J., Giambelluca, T. W., Rezende, E. L., Waite, M., & Niinemets, Ü. (2010). Faster returns on 'leaf economics' and different biogeochemical niche in invasive compared with native plant species. *Global Change Biology, 16*(8), 2171-2185.
Pesendorfer, M. B., Sillett, T. S., Koenig, W. D., & Morrison, S. A. (2016). Scatter-hoarding corvids as seed dispersers for oaks and pines: a review of a widely distributed mutualism and its utility to habitat restoration. *The Condor, 118*(2), 215-237.
Pörtner, H. O., Roberts, D. C., Adams, H., Adler, C., Aldunce, P., Ali, E., Begum, R. A., Betts, R., Kerr, R. B., & Biesbroek, R. (2022). Climate change 2022: Impacts, adaptation and vulnerability. *IPCC Sixth Assessment Report*.
Purves, D. W., Zavala, M. A., Ogle, K., Prieto, F., & Benayas, J. M. R. (2007). Environmental heterogeneity, bird-mediated directed dispersal, and oak woodland dynamics in Mediterranean Spain. *Ecological Monographs, 77*(1), 77-97.
R Core Team. (2015). R: A language and environment for statistical computing: Vienna, Austria.
Rees, W. G., Hofgaard, A., Boudreau, S., Cairns, D. M., Harper, K., Mamet, S., Mathisen, I., Swirad, Z., & Tutubalina, O. (2020). Is subarctic forest advance able to keep pace with climate change? *Global Change Biology, 26*(7), 3965-3977.
Reich, P. B., Bermudez, R., Montgomery, R. A., Rich, R. L., Rice, K. E., Hobbie, S. E., & Stefanski, A. (2022). Even modest climate change may lead to major transitions in boreal forests. *Nature, 608*(7923), 540-545.
Reich, P. B., Sendall, K. M., Rice, K., Rich, R. L., Stefanski, A., Hobbie, S. E., & Montgomery, R. A. (2015). Geographic range predicts photosynthetic and growth response to warming in co-occurring tree species. *Nature Climate Change, 5*(2), 148-152.
Reich, P. B., Tjoelker, M. G., Walters, M. B., Vanderklein, D. W., & Buschena, C. (1998). Close association of RGR, leaf and root morphology, seed mass and shade tolerance in seedlings of nine boreal tree species grown in high and low light. *Functional Ecology, 12*(3), 327-338.
Root, T. L., Price, J. T., Hall, K. R., Schneider, S. H., Rosenzweig, C., & Pounds, J. A. (2003). Fingerprints of global warming on wild animals and plants. *Nature, 421*(6918), 57-60.
Sardans, J., Vallicrosa, H., Zuccarini, P., Farre-Armengol, G., Fernandez-Martinez, M., Peguero, G., Gargallo-Garriga, A., Ciais, P., Janssens, I. A., Obersteiner, M., Richter, A., & Peñuelas, J. (2021). Empirical support for the biogeochemical niche hypothesis in forest trees. *Nature Ecology & Evolution, 5*(2), 184-194.
Shi, L., Dech, J. P., Yao, H., Zhao, P., Shu, Y., & Zhou, M. (2019). The effects of nitrogen addition on dissolved carbon in boreal forest soils of northeastern China. *Scientific Reports, 9*(1), 1-9.
Shiyatov, S. G. (2003). Rates of change in the upper treeline ecotone in the Polar Ural Mountains. *Nature, 394*, 739-743.
Si, H. H., Meicheng. (1985). Study of yield table of Dahurian larch. *Journal of North-Eastern Forestry College, 13*(2), 48-55.
Silvertown, J. (2004). Plant coexistence and the niche. *Trends in Ecology & Evolution, 19*(11), 605-611.
Silvertown, J., Araya, Y., Gowing, D., & Cornwell, W. (2015). Hydrological niches in terrestrial plant communities: a review. *Journal of Ecology, 103*(1), 93-108.
Sittaro, F., Paquette, A., Messier, C., & Nock, C. A. (2017). Tree range expansion in eastern North America fails to keep pace with climate warming at northern range limits. *Global Change Biology, 23*(8), 3292-3301.
Solarik, K. A., Cazelles, K., Messier, C., Bergeron, Y., & Gravel, D. (2020). Priority effects will impede range shifts of temperate tree species into the boreal forest. *Journal of Ecology, 108*(3), 1155-1173.
Su, Y., Guo, Q., Hu, T., Guan, H., Jin, S., An, S., Chen, X., Guo, K., Hao, Z., & Hu, Y. (2020). An updated vegetation map of China (1: 1000000). *Science Bulletin, 65*(13), 1125-1136.
Sun, H. (1998). *The forests of the Greater Khing'anling Mountains and climate change* [Master's thesis]. Northeast Forestry University.

Taylor, A. R., Boulanger, Y., Price, D. T., Cyr, D., McGarrigle, E., Rammer, W., & Kershaw, J. A. (2017). Rapid 21st century climate change projected to shift composition and growth of Canada's Acadian Forest Region. *Forest Ecology and Management*, *405*, 284-294.

Tedersoo, L., Bahram, M., & Zobel, M. (2020). How mycorrhizal associations drive plant population and community biology. *Science*, *367*(6480), eaba1223.

Tyree, M. T., Snyderman, D. A., Wilmot, T. R., & Machado, J.-L. (1991). Water relations and hydraulic architecture of a tropical tree (Schefflera morototoni) data, models, and a comparison with two temperate species (Acer saccharum and Thuja occidentalis). *Plant Physiology*, *96*(4), 1105-1113.

Urbina, I., Sardans, J., Grau, O., Beierkuhnlein, C., Jentsch, A., Kreyling, J., & Peñuelas, J. (2017). Plant community composition affects the species biogeochemical niche. *Ecosphere*, *8*(5), e01801.

Wall, S. V. (2001). The evolutionary ecology of nut dispersal. *The Botanical Review*, *67*(1), 74-117.

Walther, G. R., Post, E., Convey, P., Menzel, A., Parmesan, C., Beebee, T. J. C., Fromentin, J.-M., Hoegh-Guldberg, O., & Bairlein, F. (2002). Ecological responses to recent climate change. *Nature*, *416*(6879), 389-395.

Wang , C., Liu, W., & Liu, G. (2005). Study on the growth process of Mongolian oak in the Greater Khingan Mountains. *Forest By-Product and Specialty*(5), 60-61 (in Chinese).

Wang, Y., Pederson, N., Ellison, A. M., Buckley, H. L., Case, B. S., Liang, E., & Julio Camarero, J. (2016). Increased stem density and competition may diminish the positive effects of warming at alpine treeline. *Ecology*, *97*(7), 1668-1679.

Wen, L. (2019). *Morphological and histochemical characteristics of roots of 21 species of arbor in Northeast China* [Master's thesis]. Northeast Forestry University.

Williams, L. J., Butler, E. E., Cavender‐Bares, J., Stefanski, A., Rice, K. E., Messier, C., Paquette, A., & Reich, P. B. (2021). Enhanced light interception and light use efficiency explain overyielding in young tree communities. *Ecology Letters*, *24*(5), 996-1006.

Xiao, D., & Shu, W. (1988). Forest Soils and their Productive Properties in the North Great Xingan Mountains. *Chinese Journal of Ecology*, *7*(S1), 41-48 (in Chinese).

Xing, A., Du, E., Shen, H., Xu, L., de Vries, W., Zhao, M., Liu, X., & Fang, J. (2022). Nonlinear responses of ecosystem carbon fluxes to nitrogen deposition in an old-growth boreal forest. *Ecology Letters*, *25*(1), 77-88.

Xu, W. (1985). Kira's temperature indices and their application in the study of vegetation. *Chinese Journal of Ecology*, *4*(3), 35-39 (in Chinese).

Xu, W. (1986). The relation between the zonal distribution of types of vegetation and the climate in northeast China. *Chinese Journal of Plant Ecology*, *10*(4), 254-263 (in Chinese).

Xu, W., He, H., Huang, C., Duan, S., Hawbaker, T. J., Henne, P. D., Liang, Y., & Zhu, Z. (2022). Large fires or small fires, will they differ in affecting shifts in species composition and distributions under climate change? *Forest Ecology and Management*, *510*, 120131.

Yin, X., Zhou, G., Sui, X., He, Q., & Li, R. (2013). Dominant climatic factors of Quercus mongolica geographical distribution and their thresholds. *Acta Ecologica Sinica*, *33*(1), 103-109 (in Chinese).

Zhang, J., & Liu, B. (2014). Patterns of seed predation and removal of Mongolian oak (Quercus mongolica) by rodents. *Acta Ecologica Sinica*, *34*, 1205-1211 (in Chinese).

Zheng, H., Jia, S., & Hu, H. (1986). Forest fire and forest rehabilitation in the Daxingan Mountains. *Journal of North-East Forestry University*, *14*(4), 1-7 (in Chinese).

Zhou , X., Zhang, Y., Sun, H., Chai, Y., & Wang, Y. (2002). The effect on climate change on population dynamics of Quercus mongolica in North Greater Xing'an Mountain. *Acta Ecologica Sinica*, *22*, 981-985 (in Chinese).

Zhou, Y. (1991). Vegetation in Great Xing' An Mountains of China. *Science Press, Beijing*.

Supporting information

Additional supporting information can be found online.

Figure legends

Figure 1. Study area and sampling transect. (a) Location of the study region. (b) The sampled transect (Area 1 to 4) across the temperate-boreal ecotone and isolines of warmth index in the northern Greater Khingan Mountains in northeast China. The red points indicate sampling Area 1 to 4. The isolines indicate threshold warmth index (35 °*C month*) for Mongolian oak during 1920−1930 (brown) and 2010−2020 (purple), respectively. The regional vegetation map was adapted from Su et al. (2020). (c) Topography of the study region. (d) Significant increases in the warmth index during 1920−2019. The warmth index was calculated based on the sum of monthly mean temperatures > 5 °C in each year (see section 2.5 for more details), and the gray dotted line indicates a threshold of warmth index (35 °*C month*) for Mongolian oak. Note that fitted regression lines were overlapped for Area 2 and 3.

Figure 2. Migration direction and age structure of Mongolian oak in the forest plots across the temperate-boreal forest transect. (a) Migration of Mongolian oak across the temperate-boreal forest transect. (b) Age structure of Mongolian oak. The brown line shows the density curve in each frequency histogram. N indicates the number of Mongolian oak trees in each forest plot.

Figure 3. Estimated rates of migration of Mongolian oak. (a) The spatial variation of oldest tree ages of Mongolian oak across the sampling transect. The rates of migration of Mongolian oak were estimated separately based on the age of the oldest one tree (b), the oldest three trees (c), and the oldest 10 percent of all trees (d), respectively (see more details in Materials and Methods). Std indicates standard deviation. Old_1, Old_3 and Old_10% indicate the oldest one tree, the oldest three trees and the oldest 10 percent of oak trees at each forest plot, respectively. The shaded areas in (a) represent the 95% confidence intervals of the linear model fit.

Figure 4. Migration rates of trees within and across ecotones due to climatic warming. (a) Reported migration rates of temperate trees at the temperate-boreal ecotone (TBE) and (b) average tree migration rates at temperate-boreal ecotone (TBE), boreal-tundra ecotone (BTE) and alpine treelines (ALT). Species are ordered from left to right from the fastest to the slowest rate of migration. Abbreviations: Mon_oak, *Mongolian oak*; Pin_str, *Pinus strobus*; Bet_pop, *Betula populifolia*; Que_rub, *Quercus rubra*; Pic_gla, *Picea glauca*; Ace_rub, *Acer rubrum*; Ulm_ame, *Ulmus americana*; Pop_gra, *Populus grandidentata*; Bet_pub, *Betula pubescens*; Ace_sac, *Acer saccharum*; Til_ame, *Tilia americana*; Pic_mar, *Picea mariana*; Thu_occ, *Thuja occidentalis*; Fra_Nig, *Fraxinus Nigra*; Tsu_can, *Tsuga canadensis*; Pin_syl, *Pinus sylvestris*; Lar_gme, *Larix*

gmelinii; Ost_vir, *Ostrya virginiana*; Lar_sib, *Larix sibirica*. See Supplementary Table 5 for more detailed information on the rates of migration. Different letters in (b) indicate significant differences ($p<0.05$) using a one-way ANOVA with a Scheffe post hoc test. The error bar in (b) represents standard deviation.

Figure 5. Differences of height growth (a, b), WUE (c, d) and nitrogen utilization (e, f) and elementomes (g, h) between Mongolian oak and Dahurian larch and their variations across the ecotone. The ratio of height growth rate, the ratio of water-use efficiencies and the difference in foliar $\delta^{15}N$ between the two species indicate the differential acquisition/use of light, water and nitrogen, respectively. Distance represents the geographical distance of each site to Area1-1 (i.e., the start of the transect, see Section 2.2 and Table S1). The shaded areas in (b), (d), (f) and (h) represent the 95% confidence intervals of the linear model fit.

Figure 6. **The mechanisms (a) and conceptual model (b) of Mongolian oak migration under climatic warming**. The maximum rate of migration of Mongolian oak into boreal forests is ultimately limited by the propagule dispersal rate and the actual rate of migration is jointly constrained by dispersal barriers, climatic barriers, and biological barriers of resident boreal trees. S_a, S_b and S_c represent site a, site b and site c, respectively.

881 **Figure 1.**

882

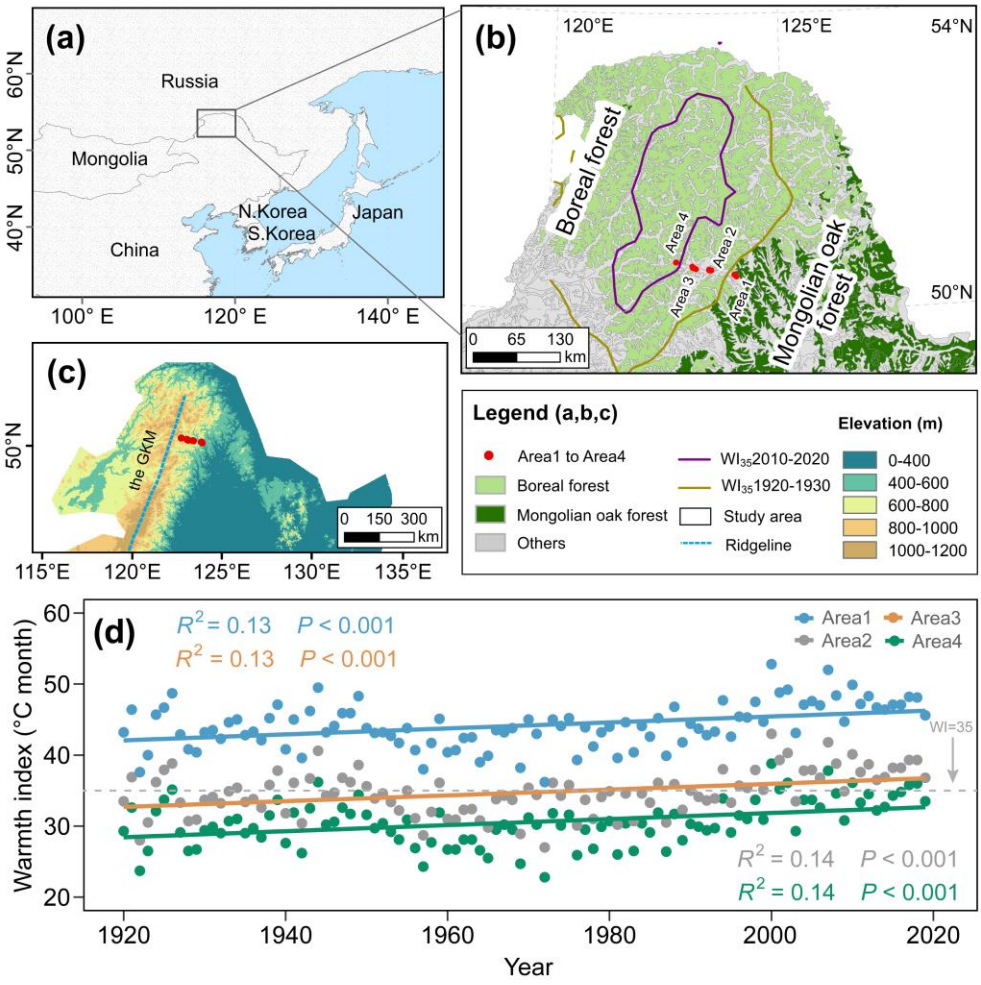

883

884

Figure 2.

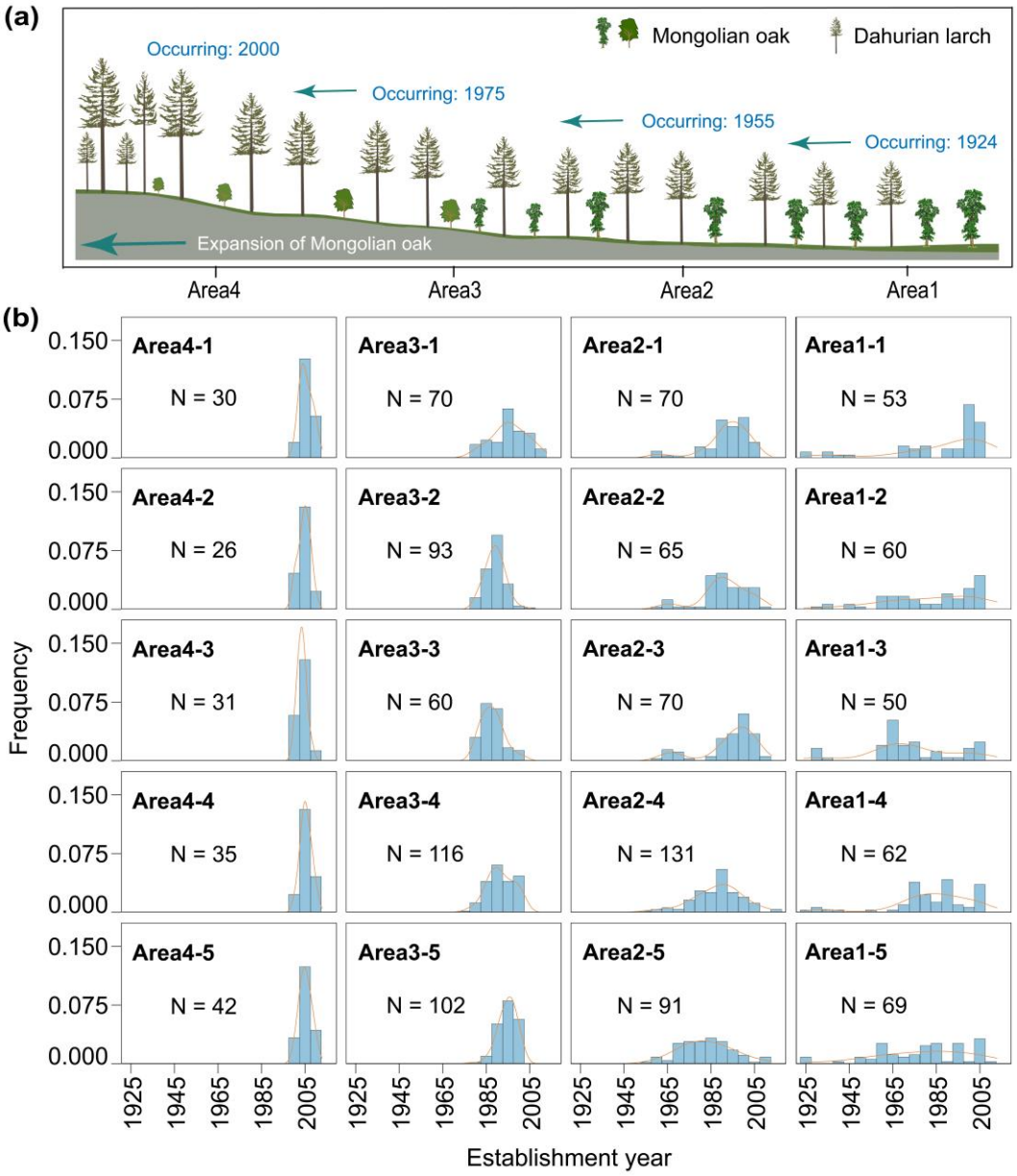
(a)
Mongolian oak
Dahurian larch
Occurring: 2000
Occurring: 1975
Occurring: 1955
Occurring: 1924
Expansion of Mongolian oak
Area4
Area3
Area2
Area1
(b)
Area4-1 N = 30
Area3-1 N = 70
Area2-1 N = 70
Area1-1 N = 53
Area4-2 N = 26
Area3-2 N = 93
Area2-2 N = 65
Area1-2 N = 60
Area4-3 N = 31
Area3-3 N = 60
Area2-3 N = 70
Area1-3 N = 50
Area4-4 N = 35
Area3-4 N = 116
Area2-4 N = 131
Area1-4 N = 62
Area4-5 N = 42
Area3-5 N = 102
Area2-5 N = 91
Area1-5 N = 69
Frequency
0.150
0.075
0.000
1925
1945
1965
1985
2005
Establishment year

889 **Figure 3.**

890

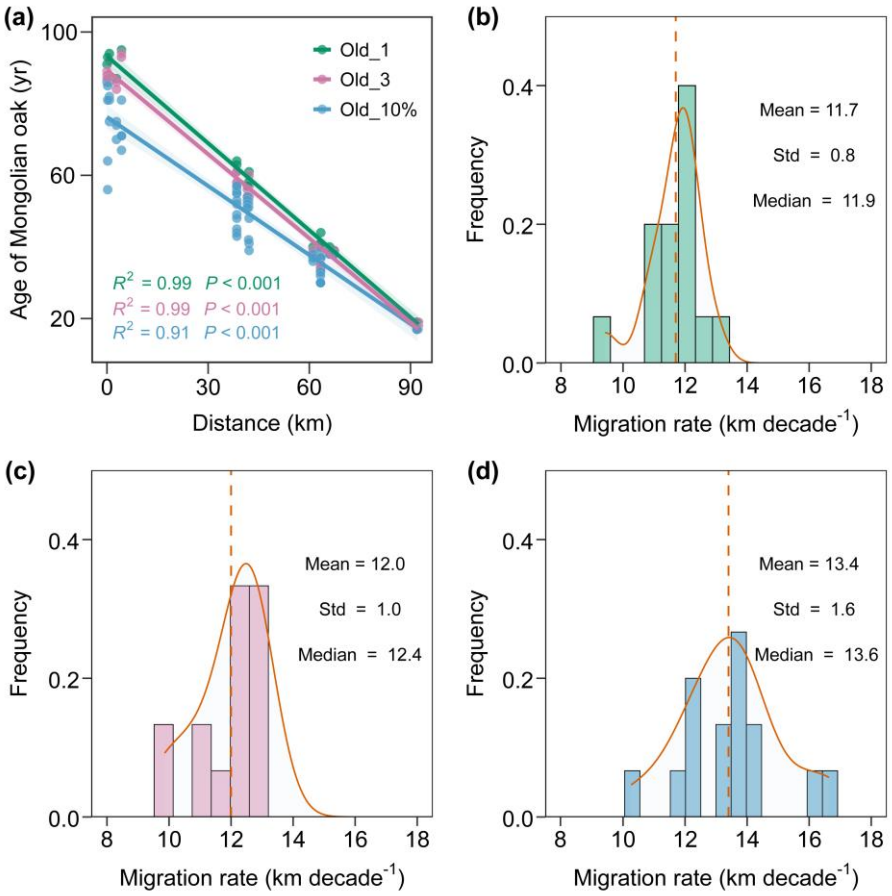

891

892

Figure 4.

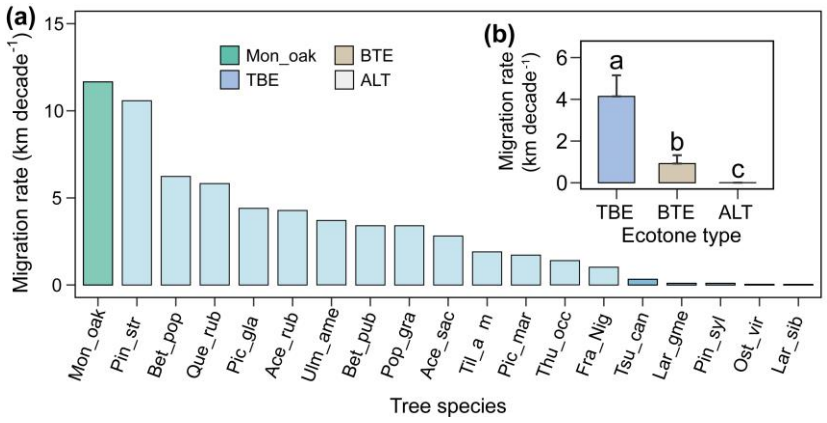
(a)
Migration rate (km decade^{-1})
15
10
5
0
Mon_oak
TBE
BTE
ALT
(b)
Migration rate (km decade^{-1})
6
4
2
0
a
b
c
TBE
BTE
ALT
Ecotone type
Mon_oak
Pin_str
Bet_pop
Que_rub
Pic_gla
Ace_rub
Ulm_ame
Bet_pub
Pop_gra
Ace_sac
Til_a_m
Pic_mar
Thu_occ
Fra_Nig
Tsu_can
Lar_gme
Pin_syl
Ost_vir
Lar_sib
Tree species

Figure 5.

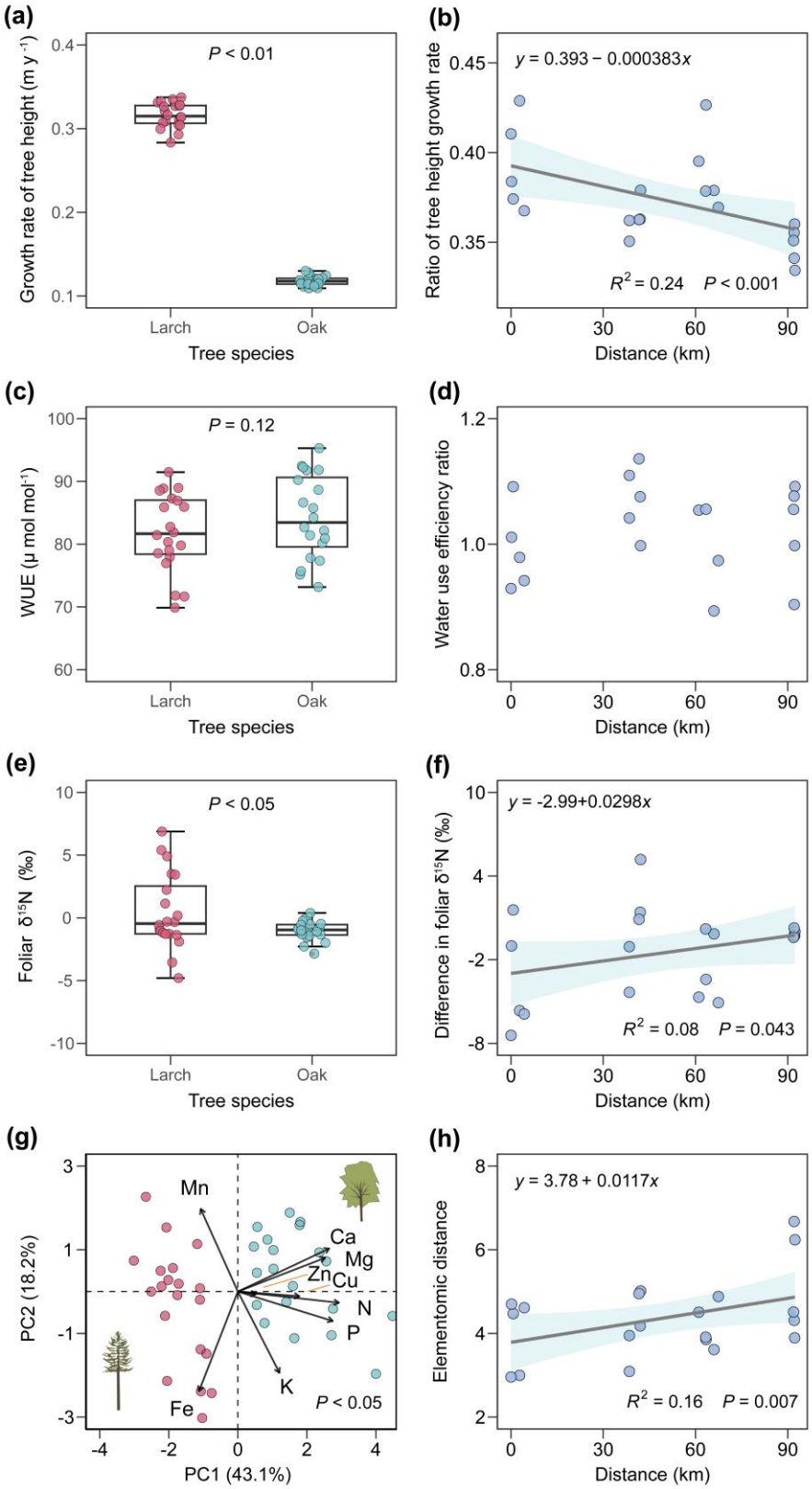
(a)
P < 0.01
Growth rate of tree height (m y-1)
Larch
Oak
Tree species
(b)
y = 0.393 − 0.000383x
Ratio of tree height growth rate
R2 = 0.24 P < 0.001
Distance (km)
(c)
P = 0.12
WUE (μ mol mol-1)
Tree species
(d)
Water use efficiency ratio
Distance (km)
(e)
P < 0.05
Foliar δ15N (‰)
Tree species
(f)
y = -2.99+0.0298x
Difference in foliar δ15N (‰)
R2 = 0.08 P = 0.043
Distance (km)
(g)
Mn
Ca
Mg
Zn
Cu
N
P
K
Fe
P < 0.05
PC2 (18.2%)
PC1 (43.1%)
(h)
y = 3.78 + 0.0117x
Elementomic distance
R2 = 0.16 P = 0.007
Distance (km)

Figure 6.

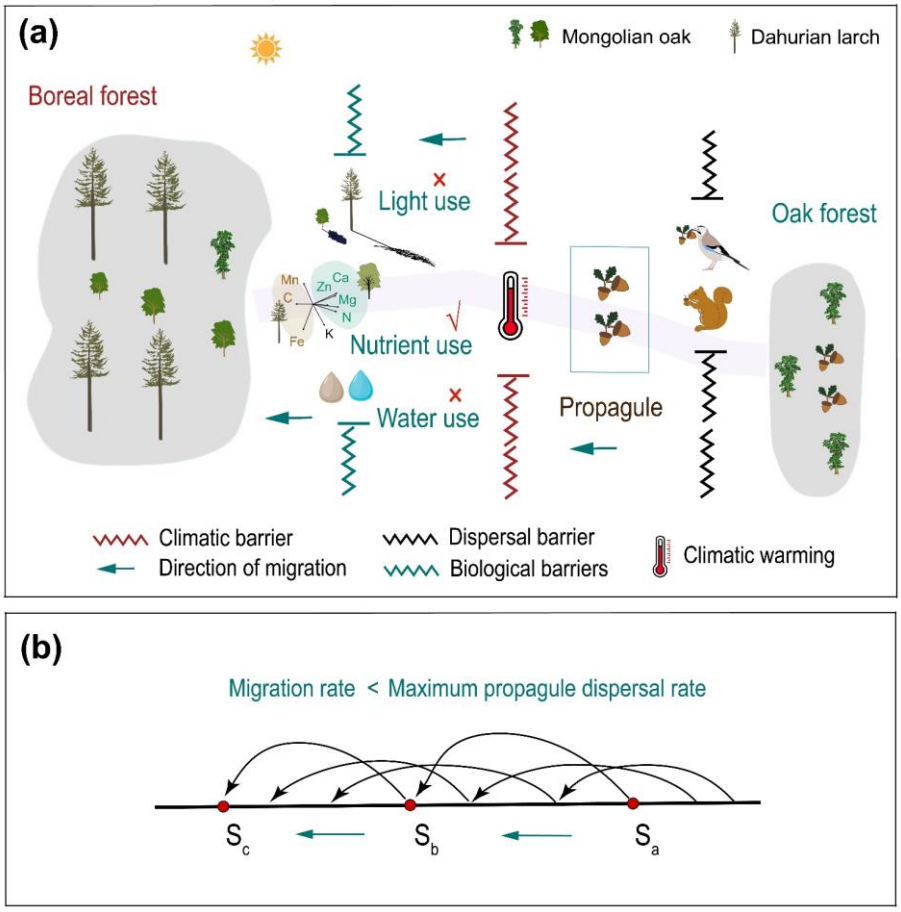
(a)
Mongolian oak
Dahurian larch
Boreal forest
Light use
Oak forest
Mn
Ca
Zn
C
Mg
N
Fe
K
Nutrient use
Water use
Propagule
Climatic barrier
Direction of migration
Dispersal barrier
Biological barriers
Climatic warming
(b)
Migration rate < Maximum propagule dispersal rate
S_c
S_b
S_a